

AUG 11 1958

RM A58C21

NACA RM A58C21

FOR REFERENCE

NACA

NOT TO BE TAKEN FROM THIS ROOM

# RESEARCH MEMORANDUM

THE STATIC LONGITUDINAL CHARACTERISTICS OF A TWISTED  
AND CAMBERED 45° SWEEPBACK WING AT MACH  
NUMBERS UP TO 0.96

By Robert I. Sammonds and Robert M. Reynolds

Ames Aeronautical Laboratory  
Moffett Field, Calif.

LIBRARY COPY

AUG 12 1958

LANGLEY AERONAUTICAL LABORATORY  
LIBRARY, NACA  
LANGLEY FIELD, VIRGINIA

NATIONAL ADVISORY COMMITTEE  
FOR AERONAUTICS

WASHINGTON

August 11, 1958



## NATIONAL ADVISORY COMMITTEE FOR AERONAUTICS

RESEARCH MEMORANDUMTHE STATIC LONGITUDINAL CHARACTERISTICS OF A TWISTED  
AND CAMBERED  $45^\circ$  SWEEPBACK WING AT MACH  
NUMBERS UP TO 0.96

By Robert I. Sammonds and Robert M. Reynolds

## SUMMARY

A  $45^\circ$  sweptback wing of aspect ratio 3, having twist and a distributed type of camber, was tested in combination with a body of fineness ratio 12.5 to determine the lift, drag, and pitching-moment characteristics. The tests were made at Mach numbers up to 0.96 at a Reynolds number of 1.5 million, and at Reynolds numbers up to 8 million at a Mach number of 0.22. The tests were conducted both with and without roughness strips near the leading edge of both the upper and lower surfaces of the wing. Comparisons have been made of these data with previously published data for a conically cambered wing having identical plan form and thickness.

The anticipated gains in maximum lift-drag ratio at high subsonic Mach numbers due to the use of a distributed type of camber rather than one concentrated near the wing leading edge (conical camber) were not realized. The maximum lift-drag ratios for the two wing-body combinations, with roughness, were nearly the same throughout the range of these tests.

The zero-lift pitching-moment coefficients for the distributed camber wing were more negative than those for the conically cambered wing. This difference in zero-lift pitching moment for the two wing-body combinations would be expected to result in drag penalties in the trimmed condition that would have an adverse effect on the lift-drag ratios for a complete model having this particular camber and twist distribution.

## INTRODUCTION

In order to increase the range of airplanes incorporating sweptback wings, attempts have been made to reduce the drag due to lift of the wing

by employing various types of camber. A conical type of camber (camber concentrated near the wing leading edge, as suggested in ref. 1) was successfully used in reference 2 on a  $45^\circ$  sweptback wing of aspect ratio 3.

Section data presented in reference 3 indicate that improvements in lift-drag ratio may be obtained at high subsonic Mach numbers by a more uniform chordwise distribution of camber rather than concentrating it near the leading edge as for the conical type of camber. However, both references 3 and 4 show that a rearward distribution of camber results in an increased negative pitching moment at zero lift which usually increases the trim drag. This zero-lift pitching moment may be avoided by a judicious choice of the spanwise variation of wing twist and by the spanwise variation of the amount and type of camber.

The present investigation was undertaken to evaluate a more uniform chordwise distribution of camber for a swept wing than is entailed with conical camber. The wing, which was tested in conjunction with a body of fineness ratio 12.5, had an aspect ratio of 3, a taper ratio of 0.4, and  $45^\circ$  sweepback of the leading edge. The camber of the wing was varied spanwise and the wing was twisted  $-5^\circ$  from the root to the tip to reduce the pitching moments at zero lift.

The tests were conducted in the Ames 12-foot pressure wind tunnel at Mach numbers from 0.60 to 0.96 at a Reynolds number of 1.5 million, and for Reynolds numbers from 3 to 8 million at a Mach number of 0.22. The tests were conducted both with and without roughness strips near the leading edge of both the upper and lower surfaces of the wing. The wing-body combination tested is identical in projected plan form to that reported in reference 2. Comparisons have been made of the data of the present investigation with similar data presented in reference 2 for a conically cambered wing having a design lift coefficient of 0.22.

#### NOTATION

A	aspect ratio, $\frac{b^2}{S}$
b	wing span
$C_D$	drag coefficient, $\frac{\text{drag}}{qS}$
$C_{D_0}$	drag coefficient at zero lift
$C_L$	lift coefficient, $\frac{\text{lift}}{qS}$
$C_{L_d}$	design lift coefficient at design Mach number of 1.0

$C_m$	pitching-moment coefficient, $\frac{\text{pitching moment}}{qS\bar{c}}$ , referred to an axis through the quarter point of the mean aerodynamic chord
$C_{m_0}$	pitching-moment coefficient at zero lift
$c$	local wing chord
$\bar{c}$	mean aerodynamic chord of wing, $\frac{\int_0^{b/2} c^2 dy}{\int_0^{b/2} c dy}$
L.E.R.	leading-edge radius
$\frac{L}{D}$	lift-drag ratio
$\left(\frac{L}{D}\right)_{\max}$	maximum lift-drag ratio
$l$	over-all length of basic body
$M$	free-stream Mach number
$q$	free-stream dynamic pressure
$R$	Reynolds number based on wing mean aerodynamic chord
$r$	local radius of body
$r_0$	maximum radius of body
$S$	wing area
$x, y, z$	Cartesian coordinates in streamwise, spanwise, and vertical directions, respectively
$\frac{dC_L}{d\alpha}$	rate of change of lift coefficient with angle of attack, $C_L = 0$
$\frac{dC_m}{dC_L}$	rate of change of pitching-moment coefficient with lift coefficient, $C_L = 0$
$\alpha$	angle of attack

- $\epsilon$  angle of twist  
 $\eta$  fraction of wing span,  $\frac{y}{b/2}$

#### Subscripts

- $l$  lower surface of wing  
 $u$  upper surface of wing  
 $LER$  leading-edge radius

#### MODEL

The model consisted of a sweptback wing mounted in the midwing position on a streamline body of revolution. The wing had an aspect ratio of 3, a leading-edge sweepback of  $45^\circ$ , a taper ratio of 0.40, and a maximum thickness of approximately 5 percent in streamwise planes. A sketch of the projected plan form of the model, showing the basic model dimensions, is presented in figure 1. Figure 1 gives the equation of the Sears-Haack body coordinates (designed to have minimum wave drag for given volume) and shows the cutoff at the rear of the body to accommodate the sting and the four-component strain-gage balance used to measure the forces and moments.

The wing consisted of NACA 64A006 sections perpendicular to the quarter-chord line of the swept airfoil sections with a leading-edge modification consisting of an increase in the nose radii as shown in figure 2. This leading-edge modification is identical to that used for the wings reported in reference 2.

The central portion of the wing (38.26 to 70.71 percent of the semispan) was cambered on the basis of an  $a = 0.8$  (modified) mean line and a design lift coefficient of 0.2. To alleviate the large negative zero-lift pitching moments resulting from the use of this type mean line, two steps were taken: the root and tip sections of the wing were cambered using one-third of an NACA 230 mean line (design lift coefficient of 0.1) and the wing was twisted  $-5^\circ$  (see fig. 3) from root to tip. The wing was smoothly faired between the root and 38.26 percent of the semispan and between 70.71 percent of the semispan and the tip in order to avoid any abrupt discontinuities in the wing surface due to the differences in camber. This effectively results in some intermediate type of camber between the 0 and 38.26 percent stations and between the 70.71 and 100 percent stations. The resultant theoretical zero-lift pitching-moment coefficient for this wing was estimated to be approximately  $-0.01$  at low speeds.

The coordinates for the cambered wing, based on the projected planform chord, are given in table I.

#### TESTS AND PROCEDURES

The lift, drag, and pitching-moment characteristics of the  $45^\circ$  sweptback wing were determined for a range of angles of attack for Reynolds numbers of 3, 6, and 8 million at a Mach number of 0.22, for Reynolds numbers of 1.5 and 2.83 million at a Mach number of 0.60, and for Mach numbers from 0.80 to 0.96 at a Reynolds number of 1.5 million.

These tests were conducted both with and without roughness strips placed along conical rays near the leading edge of both the upper and lower surfaces of the wing (see fig. 1). These roughness strips consisted of number 60 Carborundum grit imbedded in Vulcalock.

#### CORRECTIONS TO DATA

The data presented herein have been reduced to standard NACA coefficient form. The pitching-moment coefficients are referred to an axis through the quarter point of the mean aerodynamic chord.

The drag coefficient and angle of attack have been corrected by the method of reference 5 for the induced effects of the tunnel walls resulting from lift on the model. The following corrections were added to the measured values:

$$\Delta\alpha = 0.16 C_L, \text{ deg}$$

$$\Delta C_D = 0.00279 C_L^2$$

The induced effects of the tunnel walls on the pitching moment were calculated and found to be negligible.

Corrections were also applied to the data to take account of the constriction (blockage) effects of the tunnel walls (ref. 6) and the inclination of the tunnel air stream. At a Mach number of 0.90, the blockage correction amounted to an increase of less than 1 percent in the measured values of Mach number and dynamic pressure. The correction for the air-stream inclination was  $0.1^\circ$  for all test conditions.

The drag data were adjusted to correspond to a base pressure equal to free-stream static pressure.

## RESULTS AND DISCUSSION

The lift, drag, and pitching-moment data for the wing-body combination, both with and without roughness strips near the leading edge of both the upper and lower surfaces of the wing, are presented in figures 4 to 6. In figure 4, the drag data have been presented in the form  $C_D - (C_L^2/\pi A)$  for plotting convenience. The variation of the total drag coefficient ( $C_D$ ) with Reynolds number and Mach number for constant lift coefficients is shown in figures 7 and 8, respectively. Included in figures 7 and 8 are comparable data from reference 2 for a conically cambered wing having a design lift coefficient of 0.22 at a design Mach number of 1.0. The lift-drag ratios for the wing-body combination of this investigation, both with and without roughness strips, are presented in figures 9 and 10. The maximum lift-drag ratios and the lift coefficients for maximum lift-drag ratio are presented in figures 11 and 12 as a function of Reynolds number and Mach number, respectively. Also included in figures 11 and 12 are comparable data for the conically cambered ( $C_{Ld} = 0.22$ ) wing of reference 2 and for the theoretical conditions of full leading-edge suction and no leading-edge suction.<sup>1</sup> The zero-lift pitching-moment coefficients and the slopes of the lift and pitching-moment curves, near zero lift, are presented in figures 13 and 14 as a function of Reynolds number and Mach number, respectively, for both cambered wings.

At the low Reynolds numbers of this investigation and with aerodynamically smooth surfaces, the boundary layer on the model at 0° angle of attack would probably be largely laminar. As a result, sizable changes in skin friction would result from a forward chordwise shift in the region of boundary-layer transition with increasing angle of attack. In order to reduce the changes in skin friction on the model due to lift coefficient and Reynolds number, an effort was made to fix the location of the boundary-layer transition by placing roughness strips along conical rays near the leading edge of both the upper and lower surfaces of the wing. Although no attempt was made to determine whether or not the roughness strips actually fixed transition near the wing leading edge, it is felt that data for the wing with roughness are more nearly representative of full-scale conditions.

Comparison of the results of this investigation with those for the wing of identical plan form and thickness ratio but incorporating a conical type of camber ( $C_{Ld} = 0.22$ , ref. 2) shows that with roughness added

---

<sup>1</sup>The formulas used to estimate the drag coefficients for the theoretical conditions of full leading-edge suction (elliptic loading) and no leading-edge suction are  $C_D = C_{D_0} + \frac{C_L^2}{\pi A}$  and  $C_D = C_{D_0} + \frac{C_L^2}{(dC_L/d\alpha)57.3}$ , respectively, where  $C_{D_0}$  is the drag at zero lift of the plane (uncambered) wing obtained from reference 2.

(near the wing leading edge) the maximum lift-drag ratios (figs. 11 and 12) were nearly the same for both wing-body combinations. Thus, the anticipated gains in maximum lift-drag ratio at high subsonic Mach numbers due to the use of a distributed type of camber rather than one concentrated near the wing leading edge were not realized. It should be noted, however, that the design lift coefficient ( $C_{L_d}$ ) for the distributed camber wing is somewhat smaller than that for the conically cambered wing. As was anticipated, the wing with distributed camber had larger negative pitching moments at zero lift than did the conically cambered wing, and for this very reason it is doubtful whether larger amounts of distributed camber would be acceptable. It can be seen from figures 13 and 14 that the zero-lift pitching-moment coefficients varied from -0.013 to -0.037 for the wing with distributed camber and from -0.003 to -0.015 for the wing with conical camber. As a result of this difference in the zero-lift pitching moments for the two wing-body combinations, it would be expected that the wing with distributed camber when trimmed would have additional drag penalties that would have an adverse effect on the lift-drag ratios for a complete model having this particular camber and twist distribution.

The drag data presented in figures 7 and 8 show that the differences in drag for the two wing-body combinations were generally small for the highest Reynolds number of figure 7 and for the Mach number range of figure 8.

The lift and pitching-moment data presented in figures 13 and 14 show that the changes in the lift and pitching-moment curve slopes with Reynolds number and Mach number were about the same for the two wing-body combinations.

## CONCLUSIONS

Data have been presented showing the effect of Mach number and Reynolds number on the lift, drag, and pitching-moment characteristics of a  $45^\circ$  sweptback wing of aspect ratio 3 having twist and a distributed type of camber. Comparison has been made of these data with comparable data for a wing of identical plan form and thickness ratio but incorporating a conical type of camber. The results of this investigation showed:

1. The anticipated gains in maximum lift-drag ratio at high subsonic Mach numbers due to the use of a distributed type of camber rather than one concentrated near the wing leading edge (conical camber) were not realized. The maximum lift-drag ratios for the distributed camber and conical-camber wing-body combinations, with roughness, were nearly the same throughout the range of these tests.

2. The zero-lift pitching-moment coefficients for the distributed camber wing were more negative than those for the conically cambered wing. This difference in zero-lift pitching moment for the two wing-body combinations would be expected to result in drag penalties when trimmed that would have an adverse effect on the lift-drag ratios for a complete model having this particular distribution of camber and twist.

Ames Aeronautical Laboratory  
National Advisory Committee for Aeronautics  
Moffett Field, Calif., Mar. 21, 1958

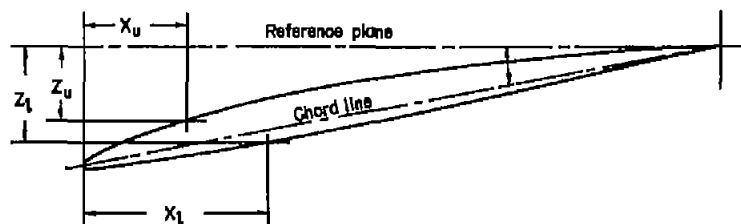
#### REFERENCES

1. Hall, Charles F.: Lift, Drag, and Pitching Moment of Low-Aspect-Ratio Wings at Subsonic and Supersonic Speeds. NACA RM A53A30, 1953.
2. Sammonds, Robert I., and Reynolds, Robert M.: The Effect of Conical Camber on the Static Longitudinal, Lateral, and Directional Characteristics of a  $45^\circ$  Sweptback Wing at Mach Numbers up to 0.96. NACA RM A56D02, 1956.
3. Summers, James L., and Treon, Stuart L.: The Effects of Amount and Type of Camber on the Variation With Mach Number of the Aerodynamic Characteristics of a 10-Percent-Thick NACA 64A-Series Airfoil Section. NACA TN 2096, 1950.
4. Stivers, Louis S., Jr.: Effects of Subsonic Mach Number on the Forces and Pressure Distributions on Four NACA 64A-Series Airfoil Sections at Angles of Attack as High as  $28^\circ$ . NACA TN 3162, 1954.
5. Glauert, H.: The Elements of Aerofoil and Airscrew Theory. The MacMillan Co., N.Y., 1943, p. 191.
6. Herriot, John G.: Blockage Corrections for Three-Dimensional-Flow Closed-Throat Wind Tunnels, With Consideration of the Effect of Compressibility. NACA Rep. 995, 1950. (Supersedes NACA RM A7B28)

TABLE I.- WING COORDINATES  
[Coordinates in inches]

Station 0				Station 2.700				Station 6.200				Station 11.456				Station 16.202			
$X_1$	$Z_1$	$X_2$	$Z_2$	$X_1$	$Z_1$	$X_2$	$Z_2$	$X_1$	$Z_1$	$X_2$	$Z_2$	$X_1$	$Z_1$	$X_2$	$Z_2$	$X_1$	$Z_1$	$X_2$	$Z_2$
0	0	0	0	0	-0.090	0	-0.090	0	-0.207	0	-0.207	0	-0.382	0	-0.382	0	-0.540	0	-0.540
.099	.078	.109	-.065	.088	-.010	.099	-.156	.074	-.123	.086	-.273	.092	-.307	.067	-.442	.033	-.480	.050	-.588
.150	.096	.160	-.076	.133	.006	.145	-.169	.112	-.111	.126	-.281	.081	-.296	.097	-.447	.082	-.471	.071	-.590
.292	.185	.266	-.091	.226	.033	.240	-.179	.192	-.088	.207	-.292	.140	-.277	.157	-.493	.092	-.456	.113	-.592
.507	.181	.523	-.116	.495	.064	.472	-.200	.388	-.042	.405	-.310	.286	-.240	.306	-.463	.193	-.424	.217	-.594
1.014	.299	1.030	-.147	.911	.156	.928	-.226	.777	.063	.796	-.329	.575	-.183	.599	-.470	.394	-.375	.420	-.589
1.514	.314	1.526	-.171	1.359	.209	1.376	-.244	1.159	.074	1.181	-.338	.661	-.138	.686	-.470	.592	-.336	.619	-.581
2.006	.355	2.013	-.193	1.802	.250	1.815	-.258	1.537	.114	1.558	-.343	1.142	-.100	1.168	-.466	.708	-.305	.815	-.571
2.965	.407	2.964	-.235	2.663	.306	2.672	-.281	2.272	.175	2.293	-.340	1.691	-.046	1.717	-.445	1.170	-.258	1.196	-.545
3.821	.435	3.826	-.272	3.496	.341	3.502	-.298	2.964	.220	3.004	-.331	2.223	-.003	2.248	-.420	1.540	-.225	1.566	-.518
4.705	.450	4.720	-.300	4.301	.366	4.306	-.310	3.673	.257	3.692	-.322	2.738	.036	2.763	-.398	1.806	-.194	1.924	-.492
5.622	.456	5.646	-.318	5.021	.382	5.025	-.315	4.342	.286	4.358	-.311	3.237	.069	3.262	-.377	2.245	-.159	2.270	-.469
6.491	.455	6.486	-.329	5.837	.390	5.821	-.315	4.969	.306	5.004	-.298	3.780	.097	3.743	-.354	2.580	-.131	2.606	-.445
7.305	.446	7.300	-.332	6.570	.390	6.573	-.310	5.617	.318	5.630	-.281	4.190	.118	4.211	-.330	2.906	-.105	2.932	-.418
8.094	.428	8.089	-.325	7.280	.381	7.282	-.296	6.226	.321	6.237	-.259	4.645	.132	4.664	-.302	3.223	-.086	3.247	-.387
8.860	.402	8.855	-.309	7.970	.364	7.971	-.276	6.817	.315	6.826	-.233	5.087	.138	5.104	-.271	3.530	-.069	3.553	-.354
9.603	.370	9.599	-.288	8.640	.340	8.640	-.252	7.391	.302	7.397	-.205	5.517	.140	5.531	-.239	3.823	-.056	3.850	-.319
10.325	.334	10.321	-.262	9.290	.312	9.290	-.224	7.949	.284	7.953	-.175	5.934	.137	5.946	-.206	4.118	-.045	4.138	-.284
11.026	.295	11.023	-.233	9.921	.280	9.921	-.195	8.490	.265	8.493	-.146	6.339	.130	6.348	-.174	4.401	-.036	4.417	-.247
11.708	.253	11.706	-.200	10.536	.244	10.535	-.163	9.017	.233	9.017	-.116	6.734	.119	6.740	-.142	4.674	-.029	4.689	-.210
12.371	.209	12.369	-.166	11.133	.206	11.131	-.132	9.529	.201	9.527	-.088	7.117	.105	7.121	-.111	4.942	-.023	4.954	-.173
13.016	.165	13.015	-.131	11.715	.165	11.712	-.101	10.028	.165	10.024	-.063	7.491	.088	7.492	-.083	5.201	-.018	5.211	-.138
13.644	.123	13.643	-.098	12.279	.123	12.277	-.075	10.511	.124	10.507	-.046	7.853	.067	7.852	-.060	5.454	-.014	5.460	-.102
14.255	.081	14.254	-.065	12.830	.082	12.828	-.050	10.982	.083	10.979	-.030	8.206	.045	8.204	-.039	5.699	-.008	5.704	-.067
14.850	.041	14.850	-.033	13.365	.041	13.364	-.025	11.440	.041	11.439	-.015	8.549	.022	8.549	-.020	5.939	-.004	5.941	-.033
15.430	.005	15.430	-.005	13.887	.005	13.887	-.005	11.887	.004	11.887	-.004	8.884	.002	8.884	-.003	6.172	.001	6.172	-.001
L.W.R.	0.029				0.029				0.035				0.050				0.057		
(x)TWR	.089				.089				.035				.050				.056		
(y)TWR	.002				-.088				-.205				-.377				-.531		
e	0°				-.36°				-1.00°				-2.46°				-5.00°		

- Notes: 1. Root and tip sections on a chord perpendicular to  $x/c = 0.31 = \text{constant}$  are NACA 64A006 airfoils on one-third of an NACA 230 mean line for  $\alpha_{tip} = 0.1$ .
2. Sections at station 6.200 and 11.456 on chords perpendicular to  $x/c = 0.31$  are NACA 64A006 sections on an  $a = 0.8$  (modified) mean line for  $\alpha_{tip} = 0.2$ .
3. Wing is twisted for linear elements with  $\alpha_{tip} = -5.00^\circ$ .
4. Wing elements are faired between given stations over the entire wing to eliminate any abrupt discontinuities due to the different combers.



1. The first part of the report is a review of the literature on the subject of the aerodynamic characteristics of airfoils with leading edge serrations. This review covers the work of other investigators in this field, including the work of the present author in a previous report (NACA RM A58C20). The review is organized into two main sections: one dealing with the aerodynamic characteristics of airfoils with leading edge serrations in the absence of a boundary layer, and the other dealing with the aerodynamic characteristics of airfoils with leading edge serrations in the presence of a boundary layer. The first section is divided into three sub-sections: one dealing with the lift and drag characteristics of airfoils with leading edge serrations, one dealing with the pitching moment characteristics of airfoils with leading edge serrations, and one dealing with the stall characteristics of airfoils with leading edge serrations. The second section is divided into two sub-sections: one dealing with the lift and drag characteristics of airfoils with leading edge serrations in the presence of a boundary layer, and one dealing with the pitching moment characteristics of airfoils with leading edge serrations in the presence of a boundary layer. The second section also includes a discussion of the effect of leading edge serrations on the stall characteristics of airfoils in the presence of a boundary layer. The review concludes with a summary of the results of the literature search and a list of references.

Equation of body coordinates

$$\frac{r}{r_0} = \left[ 1 - \left( 1 - \frac{2x}{l} \right)^2 \right]^{\frac{3}{4}}$$

Note: 1. All dimensions in inches unless otherwise noted  
 2. All wing dimensions for a projected plan form

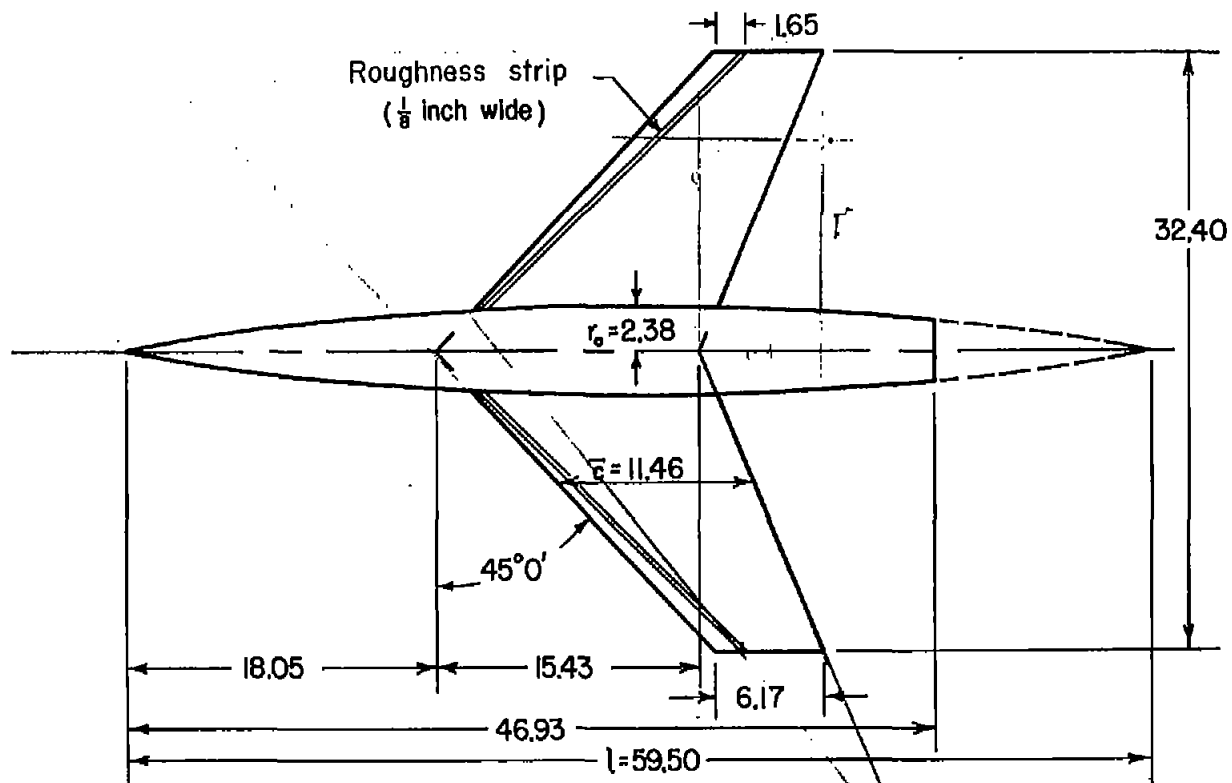


Figure 1.- Model arrangement.

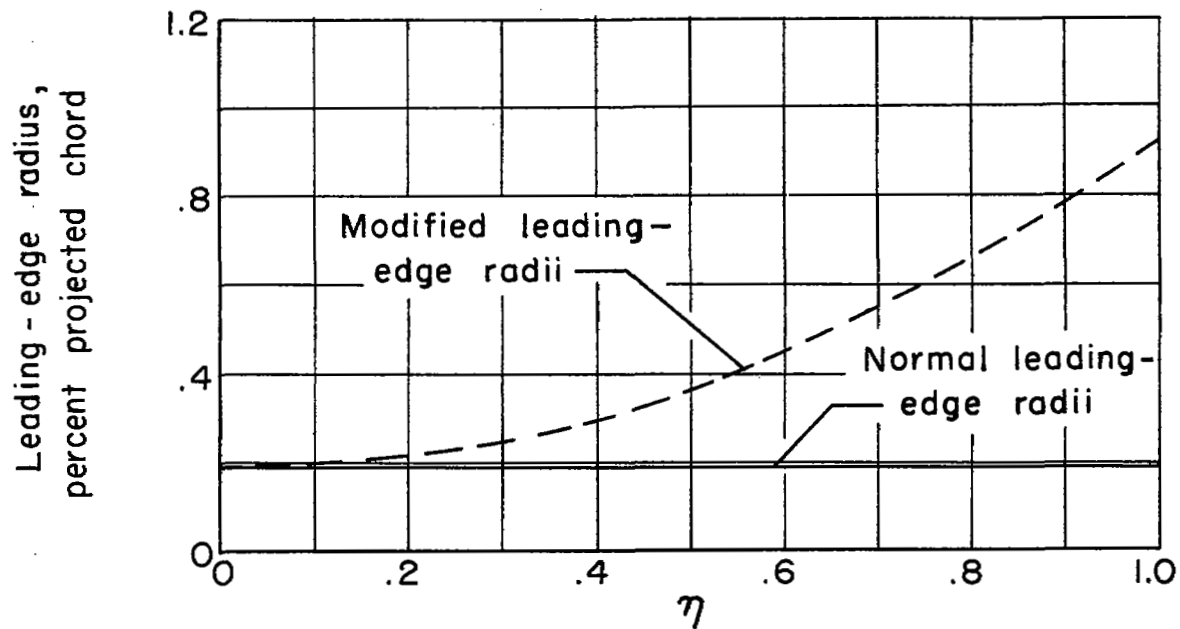


Figure 2.- Comparison of normal and modified leading-edge radii for sweptback wing.

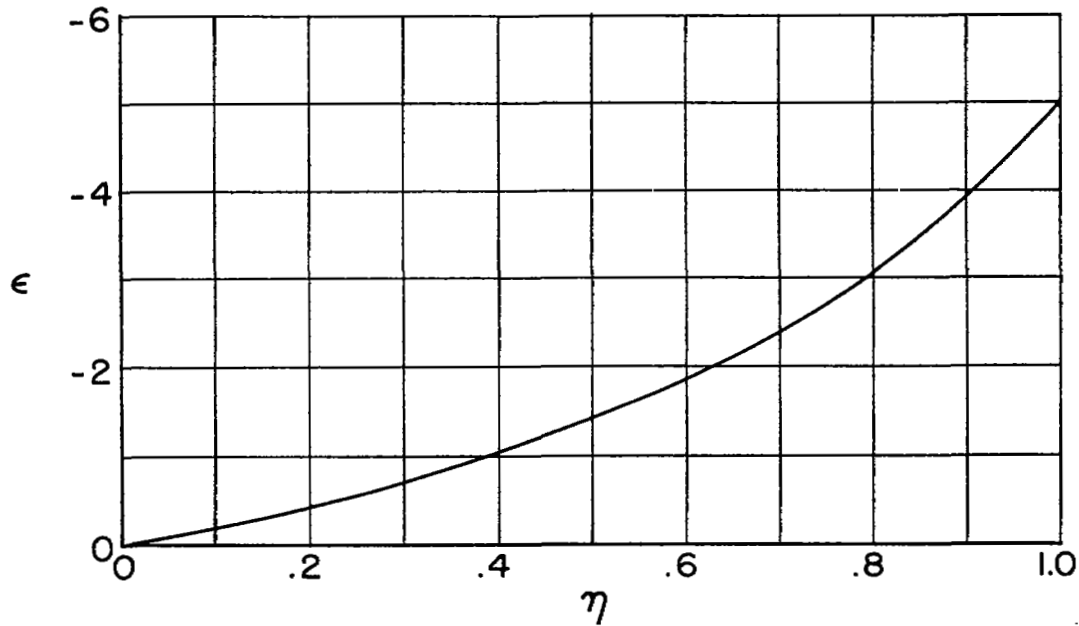
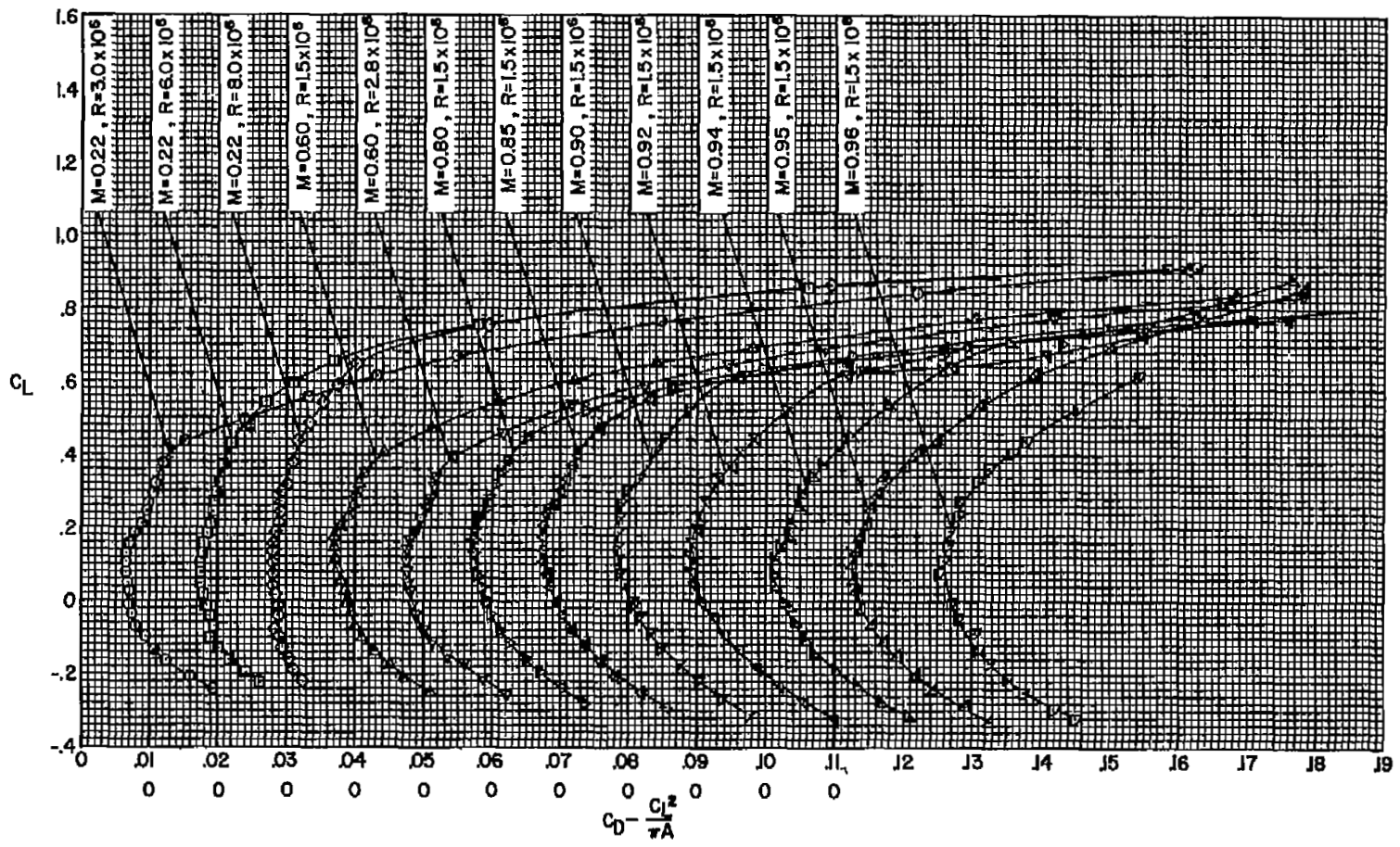
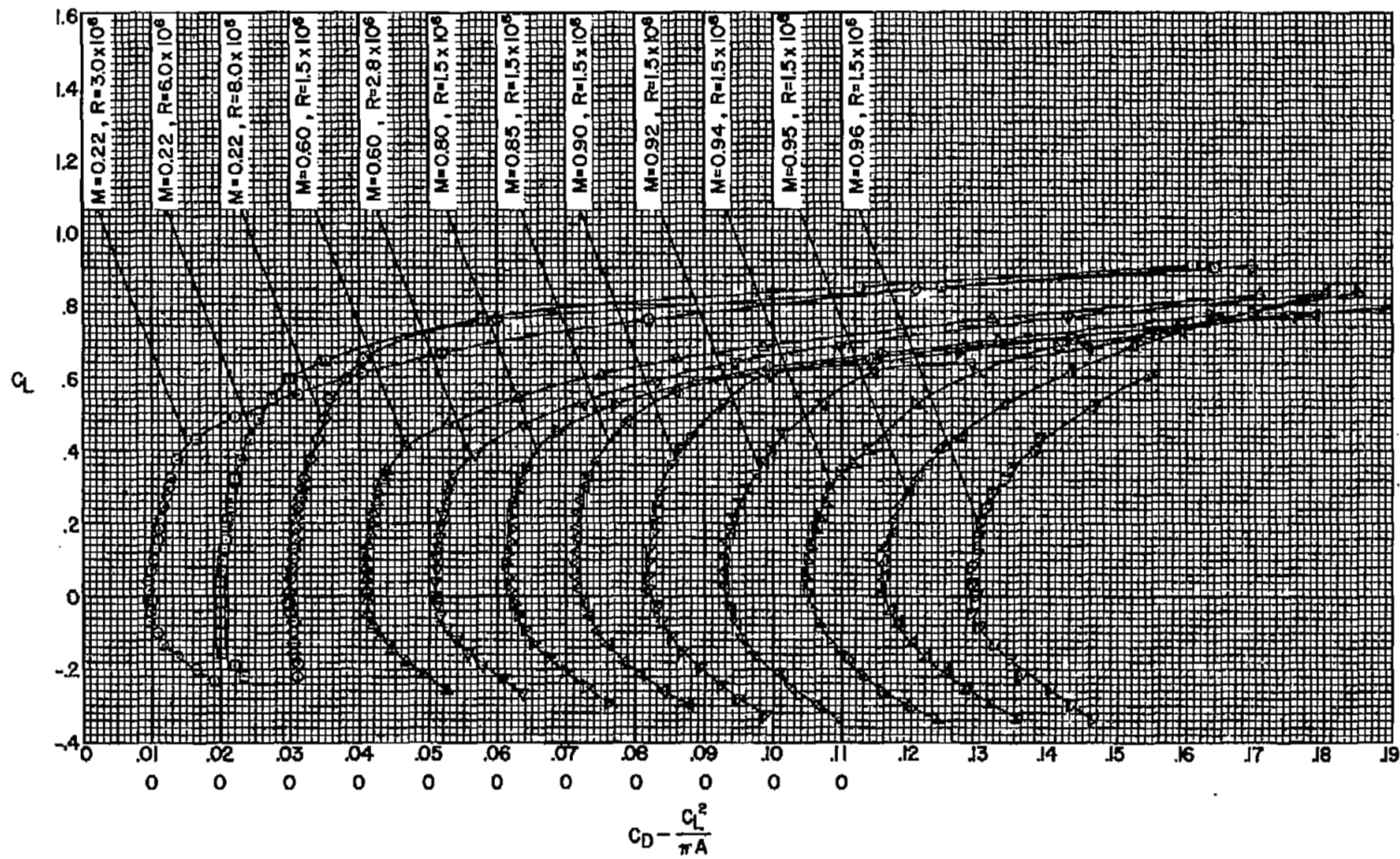


Figure 3.- Wing twist distribution.



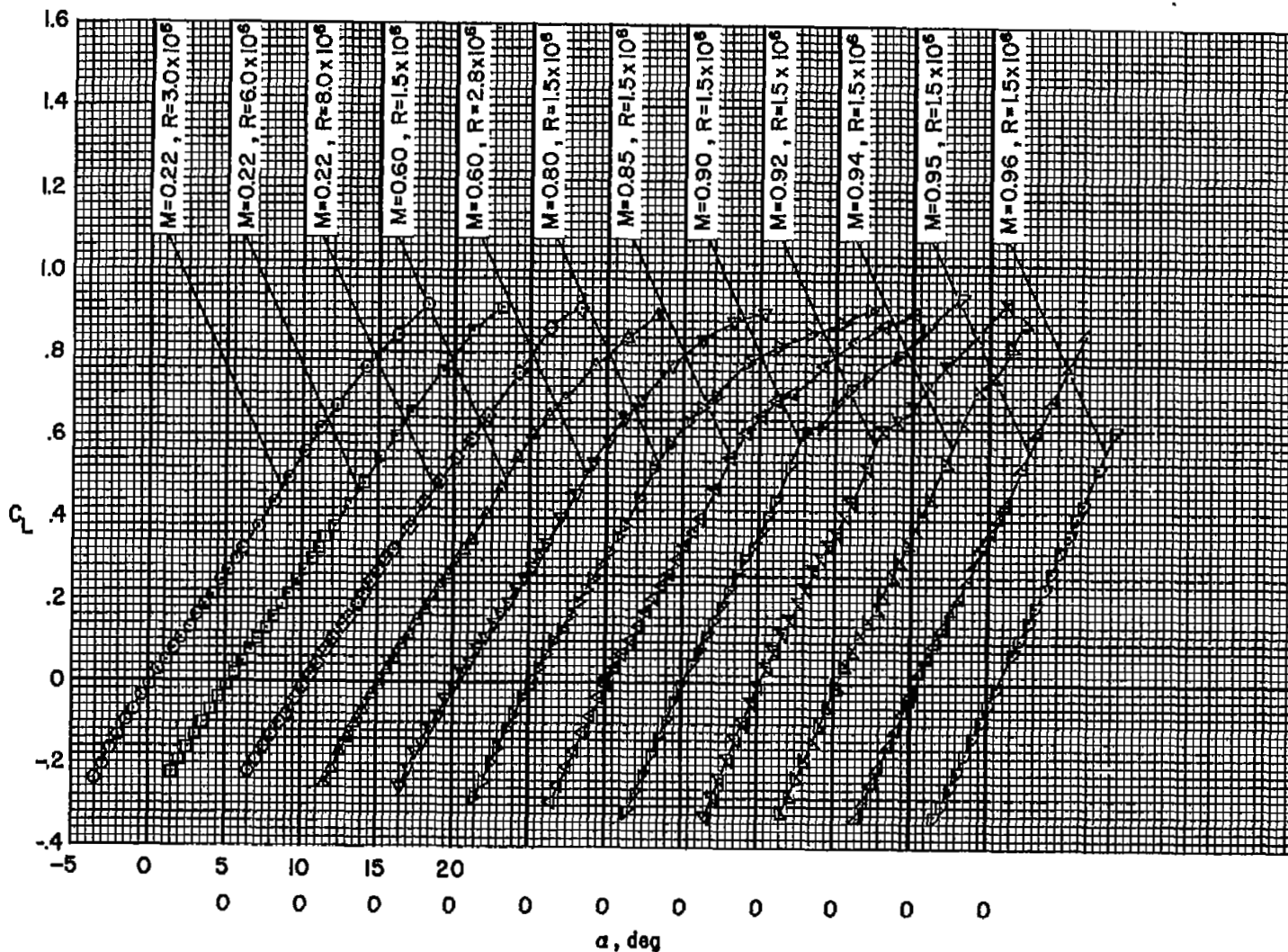
(a) Without roughness.

Figure 4.- The effect of Reynolds number and Mach number on the drag characteristics.



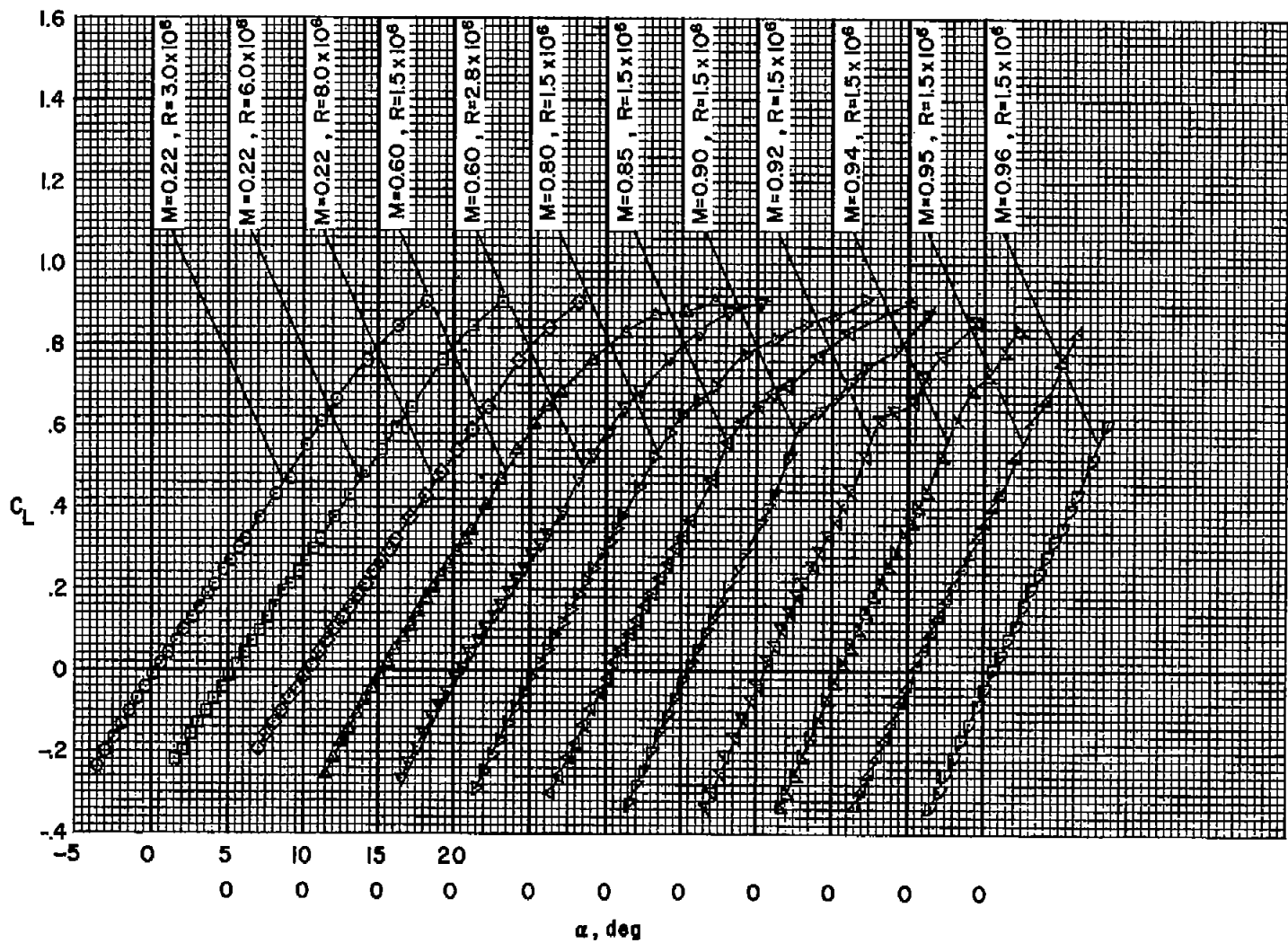
(b) With roughness.

Figure 4.- Concluded.



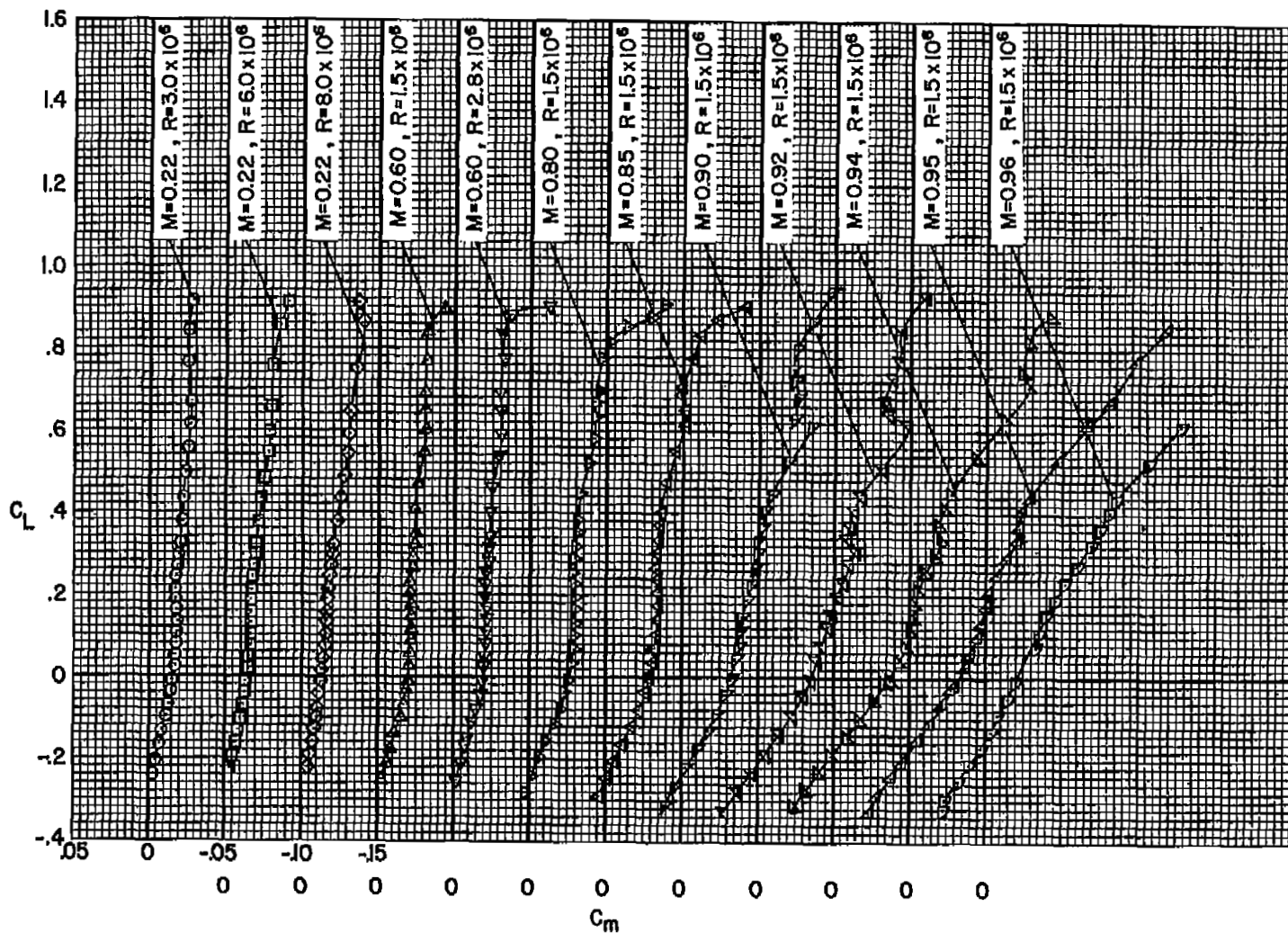
(a) Without roughness.

Figure 5.- The effect of Reynolds number and Mach number on the lift characteristics.



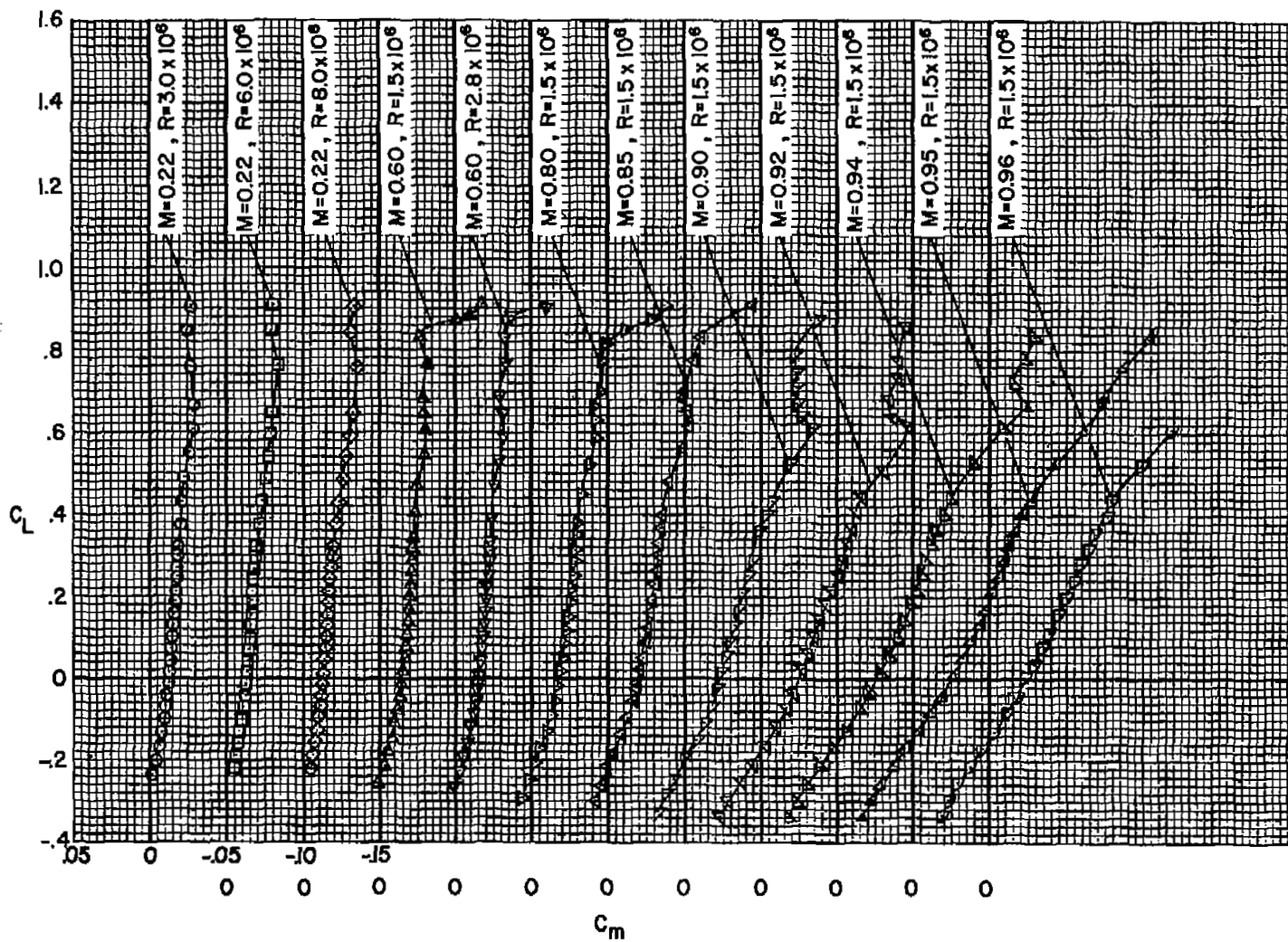
(b) With roughness.

Figure 5.- Concluded.



(a) Without roughness.

Figure 6.- The effect of Reynolds number and Mach number on the pitching-moment characteristics.



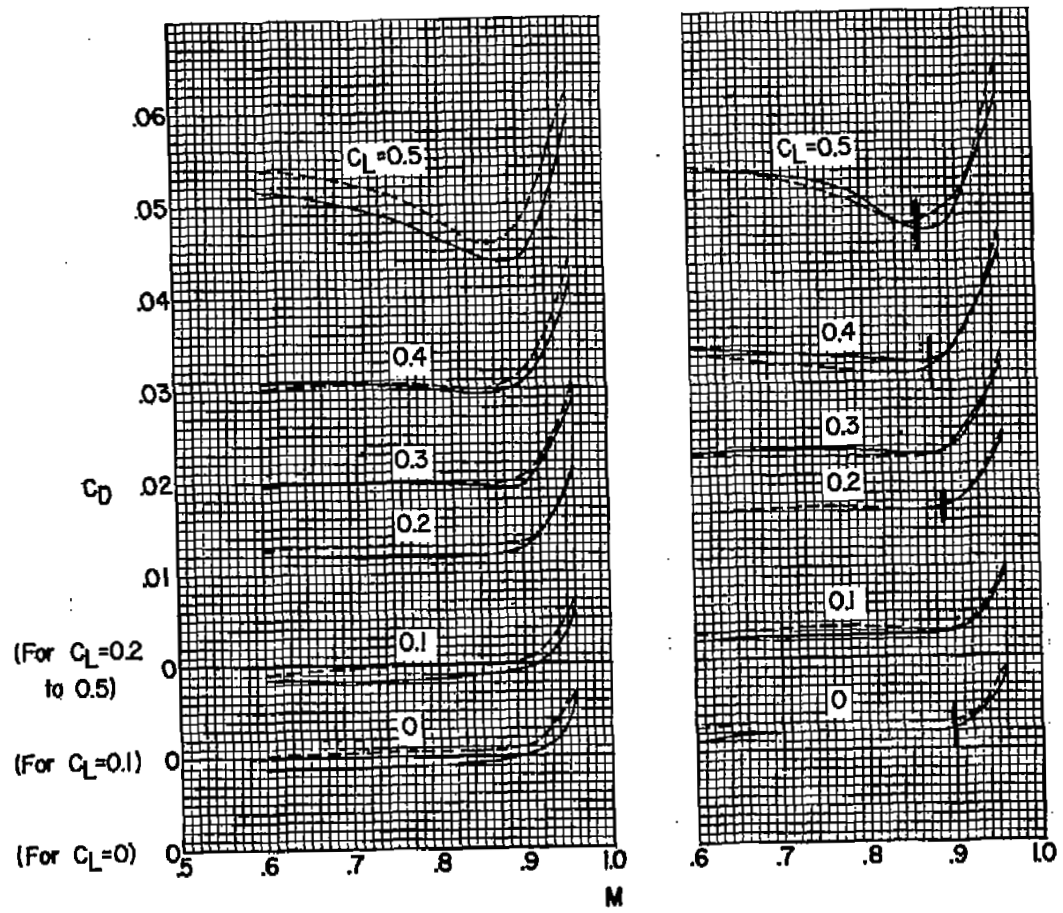
(b) With roughness.

Figure 6.- Concluded.



AA-3.0  
TLC-04

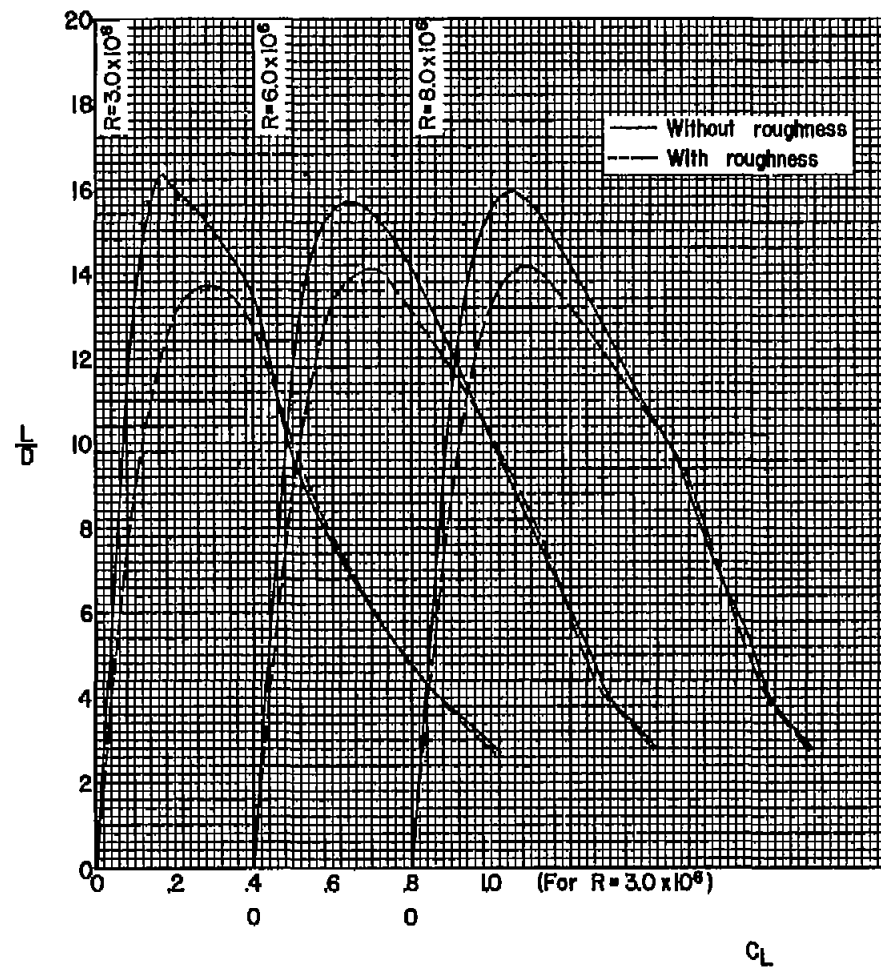
— Distributed camber  
 - - - Conical camber for  $C_{Ld}=0.22$ (ref. 2)



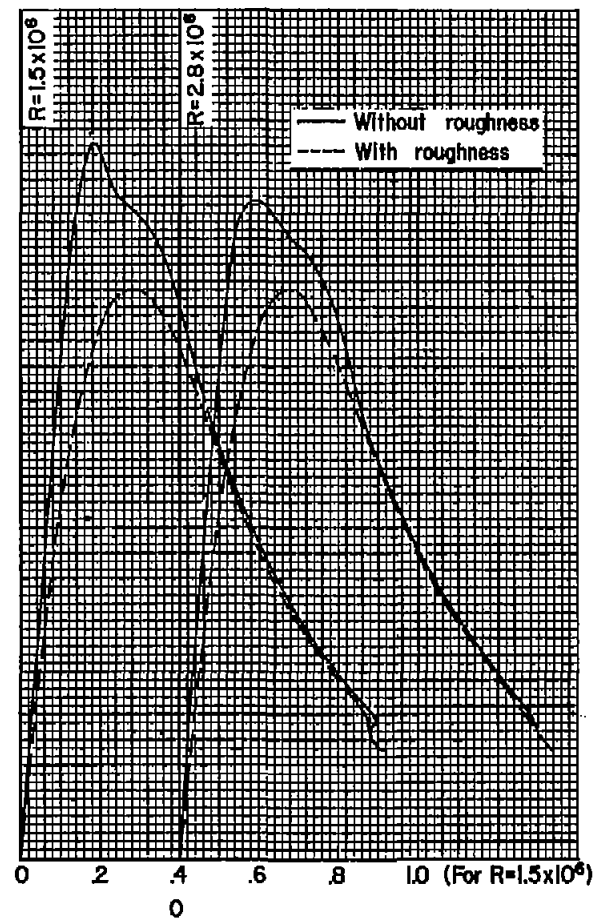
(a) Without roughness.

(b) With roughness.

Figure 8.- The variation with Mach number of the drag coefficient at constant lift coefficients;  
 $R = 1.5 \times 10^6$



(a)  $M = 0.22$



(b)  $M = 0.60$

Figure 9.- The effect of Reynolds number on the lift-drag ratios.

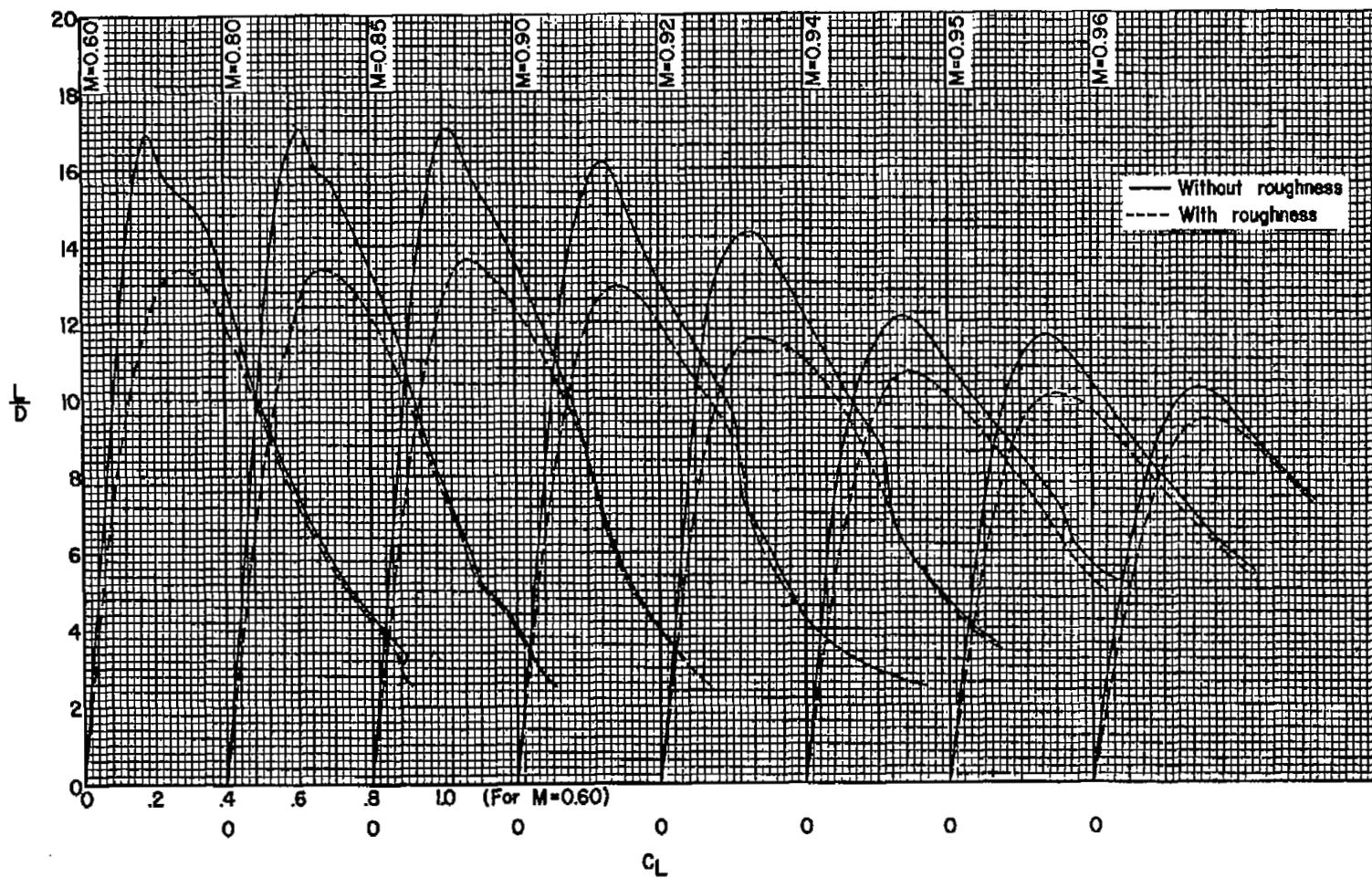


Figure 10.- The effect of Mach number on the lift-drag ratios;  $R = 1.5 \times 10^6$ .



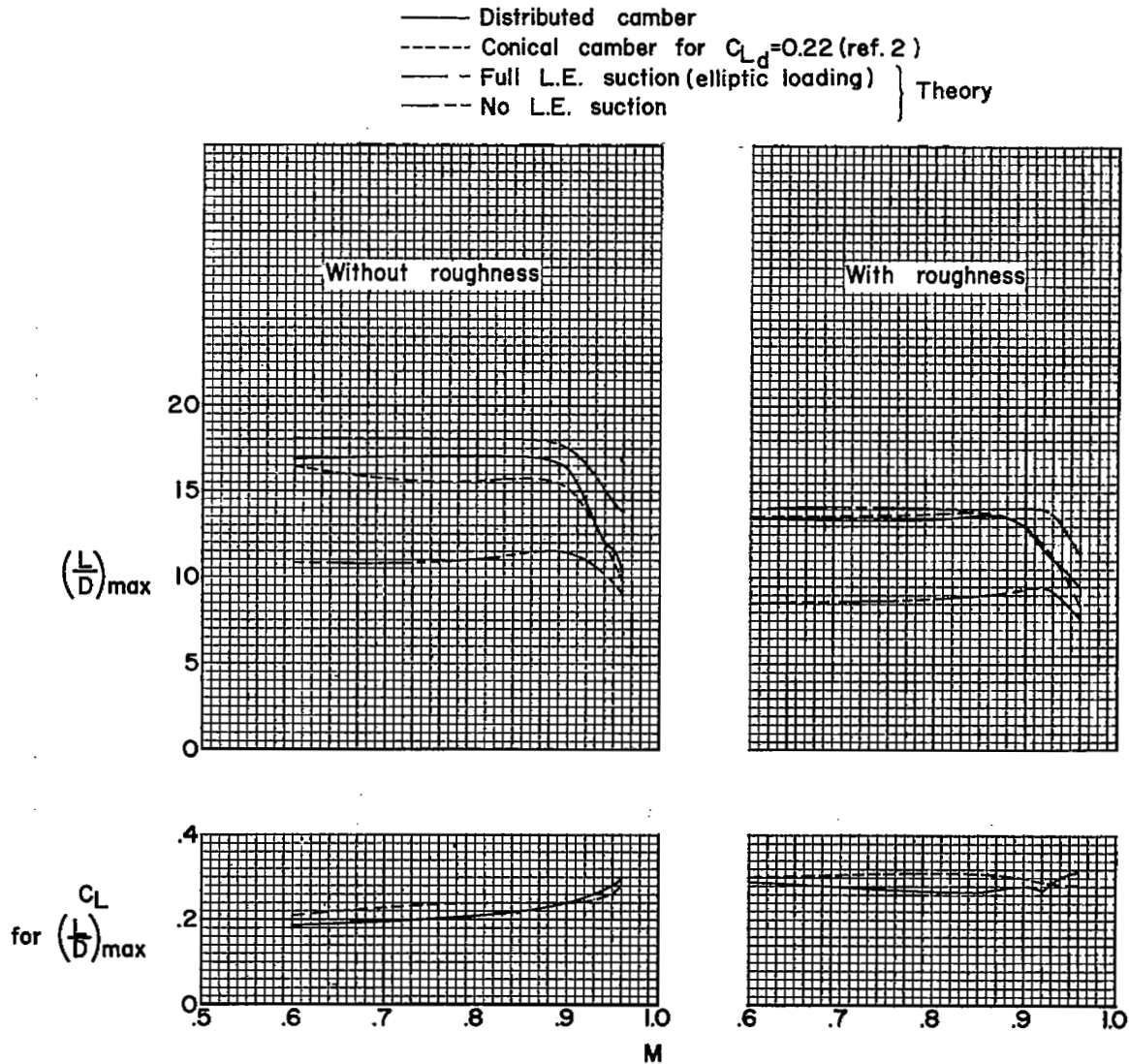


Figure 12.- The variation with Mach number of the maximum lift-drag ratios and the lift coefficients for maximum lift-drag ratios;  $R = 1.5 \times 10^6$ .



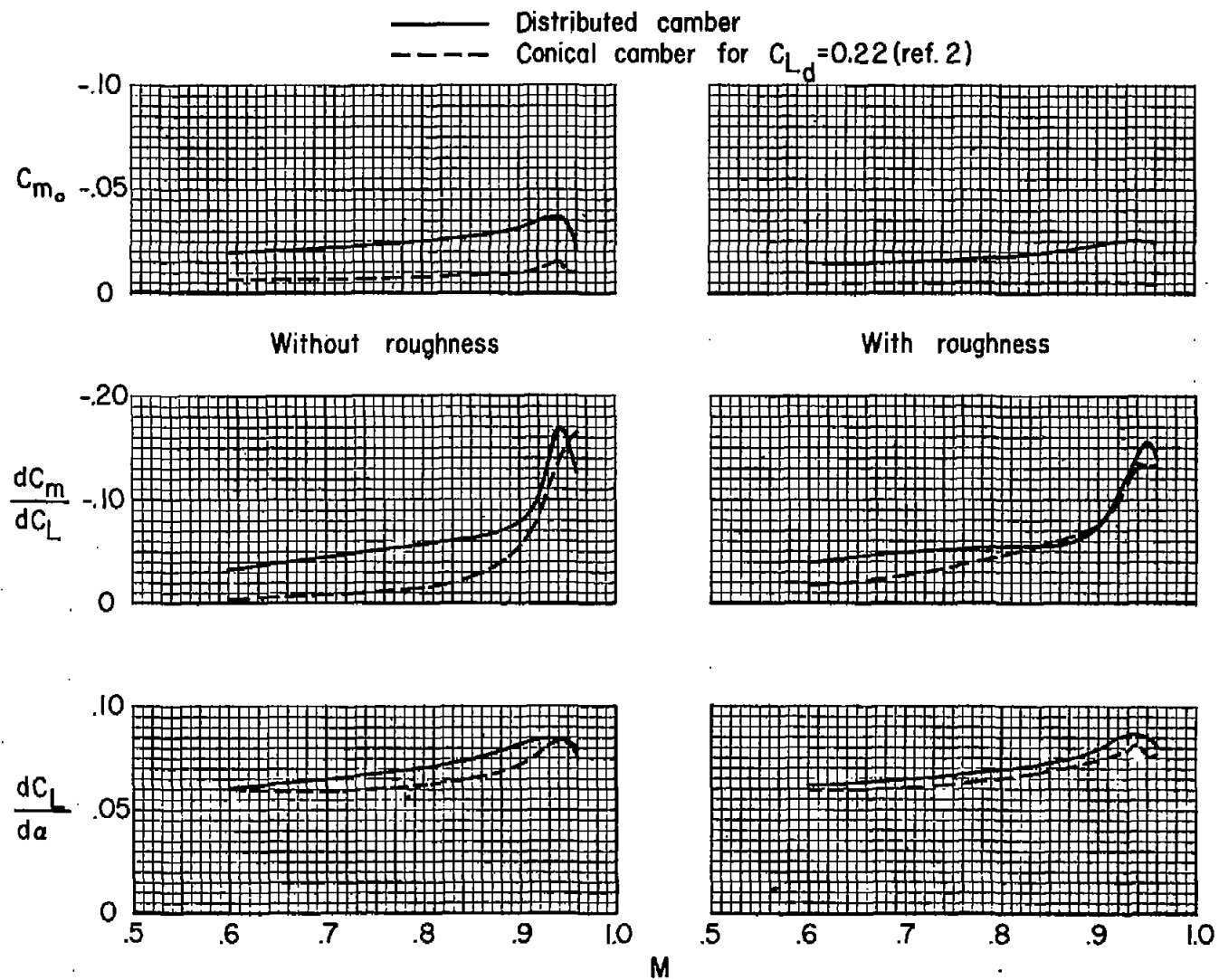


Figure 14.- The variation with Mach number of the pitching moment and the lift and pitching-moment curve slopes;  $C_L = 0$ ,  $R = 1.5 \times 10^8$ .

NASA Technical Library



3 1176 01434 9626

C  
A  
V

L  
A  
Y  
P

L  
A  
Y  
P